Cement & Concrete Composites 34 (2012) 1095–1103

Contents lists available at SciVerse ScienceDirect

Cement & Concrete Composites

journal homepage: www.elsevier.com/locate/cemconcomp

Effects of colloidal nanoSiO$_2$ on fly ash hydration

Pengkun Hou [a,b], Kejin Wang [c], Jueshi Qian [a,*], Shiho Kawashima [b], Deyu Kong [b,d], Surendra P. Shah [b]

[a] College of Materials Science and Engineering, Chongqing University, Chongqing 400045, China
[b] Department of Civil and Environmental Engineering, Northwestern University, Evanston, IL 60208, USA
[c] Department of Civil, Construction and Environmental Engineering, Iowa State University, Ames, IA 50011, USA
[d] College of Architecture and Civil Engineering, Zhejiang University of Technology, Hangzhou 310014, China

ARTICLE INFO

Article history:
Received 9 April 2012
Received in revised form 19 June 2012
Accepted 20 June 2012
Available online 27 June 2012

Keywords:
Nanosio$_2$
Fly ash
Hydration
Morphology
Coating

ABSTRACT

The influences of colloidal nanoSiO$_2$ (CNS) addition on fly ash hydration and microstructure development of cement–fly ash pastes were investigated. The results revealed that fly ash hydration is accelerated by CNS at early age thus enhancing the early age strength of the materials. However, the pozzolanic reaction of fly ash at later age is significantly hindered due to the reduced CH content resulting from CNS hydration and the hindered cement hydration, as well as due to a layer of dense, low Ca/Si hydrate coating around fly ash particles. The results and discussions explain why the cementitious materials containing nanoSiO$_2$ had a lower strength gain at later ages. Methods of mitigating the adverse effect of nanoSiO$_2$ on cement/FA hydration at later ages were proposed.

1. Introduction

Fly ash, a waste, byproduct of power plants, has been increasingly used in cement and concrete materials because of many advantages, such as reduced carbon footprint, increased flowability, decreased hydration heat, enhanced long-term strength growth, reduced shrinkage, improved durability and lower cost. Undesirably, delay in early-age strength gain of fly ash cement-based materials is often considered to be a major drawback [1–3] except for some special concrete applications, such as mass concrete [4]. To compensate for this shortcoming, many methods have been explored to accelerate the early-age hydration of fly ash–cement systems, including mechanical grinding [5], chemical activation [6], mechanochemical treatment [7] and hydrothermal treatment [8,9].

On the other hand, silica fume (SF) has been found to be very effective in accelerating cement hydration [10]. Containing over 90% SiO_2 (by weight), SF reacts with calcium hydroxide (CH) and produces additional C–S–H gel in a cement system, leading the system to a denser microstructure through its pozzolanic reaction and improving the mechanical properties as well as the durability of the hardened cementitious materials [11]. Some researches suggested that the early-age compressive strength of SF-added materials was improved significantly but sometimes, it is still lower than that of the control [11,12]. More recently, a more pozzolanic-reactive material, nanoSiO$_2$, has been used to improve the properties of cementitious materials, and it shows an excellent enhancing effects on the early-age properties [13]. Jo et al. [14] reported that 6% nanoSiO$_2$ improves the compressive strength of plain mortar by 152%, from 18.3 MPa to 46.3 MPa, at 7 days. The improvements were attributed to three reasons: (1) the acceleration effect of CNS on cement hydration, (2) pozzolanic reaction of CNS, and (3) improved particle packing of the matrix. For the pozzolan replacement cement-based materials system, some researchers [15–18] found that the physical and mechanical properties of fly ash/slag systems can be greatly enhanced. However, the results from the previous studies were largely obtained from the investigations at early ages. Although other nanoparticles were studied [19,20], nanosilica has often been the first choice due to its high pozzolanic activity.

A common characteristic of CNS and fly ash is that they both are pozzolanic materials, and both adsorb, react with, or consume, CH that is generated from cement hydration. Normally, to get a considerable improvement of strength gain, the dosage of nanoSiO$_2$ shall not be less than 5% by mass of binder [13–15,21–23]. It is estimated that a 5 g nanoSiO$_2$ addition can adsorb almost 50% of the CH produced by 100 g of cement when assuming nanoSiO$_2$ has been fully hydrated and a total of 20 g of CH can be generated, yielding a gel with a normal type of C–S–H gel with Ca/Si ratio of 1.7 [24]. Since nanoSiO$_2$ and fly ash compete in adsorbing CH and nanoSiO$_2$ is far more reactive than FA, it can be deduced that there may be a shortage of CH in a nanoSiO$_2$-added fly ash cementitious material system, thus preventing fly ash hydration at the later age, especially when the fly ash content is high.

* Corresponding author. Tel.: +86 23 65126109.
E-mail address: qianjueshi@126.com (J. Qian).

0958-9465/$ - see front matter © 2012 Elsevier Ltd. All rights reserved.
http://dx.doi.org/10.1016/j.cemconcomp.2012.06.013

Table 1
Physiochemical compositions of cement and fly ash.

Materials	Type I cement	Fly ash
SiO_2	20.2	46
Al_2O_3	4.7	17.8
Fe_2O_3	3.3	18.2
SO_3	3.3	2.59
CaO	62.9	8.4
MgO	2.7	0.95
Na_2O	/	0.59
K_2O	/	2.16
LOI	1.1	1.49
Total	98.2	98.2
Density (g/cm^3)	3.10	2.30

The present study is to verify the above-mentioned hypothesis through investigating the influence of nanoSiO_2 on fly ash hydration. In this study, mechanical properties of nanoSiO_2-added fly ash cement mortar are evaluated at both early and later ages, and the governing mechanisms of the nanoSiO_2 influence on fly ash hydration are studied. These results may provide a comprehensive explanation for mechanical behavior of a nanoSiO_2 – fly ash cementitious material system. At the same time, propositions of eliminating the adverse side effects of nanoSiO_2 on cement-based materials at later ages were raised.

2. Experimental

2.1. Materials

A type I Portland cement with Blaine fineness of 385 m^2/kg and a Type F fly ash were used in this study. The chemical compositions of cement and fly ash are shown in Table 1. To facilitate a homogeneous distribution of nanoSiO_2 in cement paste, colloidal nanoSiO_2 (CNS), instead of nanoSiO_2 powder, was used. The sodium stabilized CNS used was produced by the sol–gel technique and had an average particle size of 10 nm, pH value of 10.5, and SiO_2 content (by weight) of 99%, which were provided by the supplier [25]. The density of CNS as measured is 2.39 g/cm^3, which is comparable to that of fly ash of 2.30 g/cm^3 as listed in Table 1. Water content in CNS (60% by mass) was considered in the mix proportion calculation. The transmission electron microscopy (TEM) image of CNS and scanning electron microscopy (SEM) image of FA are shown in Fig. 1. Fig. 1(a) indicates that most of the CNS particles are well-dispersed.

2.2. Mix proportion and sample casting

Unless stated otherwise, cement pastes made with 40% (by mass) fly ash replacement with or without another 5% (% by mass of cement plus fly ash) CNS, at a water-to-binder (CNS was treated as a component of the binder) ratio of 0.4 were used throughout this study. The pastes were mixed according to ASTM C305 [26]. After mixing, samples were casted in 2 cm × 2 cm × 8 cm molds for chemistry and microscopic studies such as degree of hydration, thermogravimetric analysis (TGA), and SEM. After cured in room temperature for 1 day, the samples were demolded and cured in saturated lime water at a room temperature until testing. Pastes used for heat of hydration measurements were also mixed according to the same process.

To prepare samples for degree of hydration and TGA tests, a small core was taken from the 2 cm × 2 cm × 8 cm sample at a given curing age, and it was crushed into small pieces and immediately immersed in acetone to stop hydration and minimize carbonization. The samples were then oven-dried at 105 °C for 4 h and ground so as to pass the 100 mesh size (ca. 150 μm) sieve.

To prepare samples for SEM studies, small fractured samples were taken from the cores. They were then soaked in acetone for 3 days and dried at 80 °C for 2 h. The samples were coated with 20 nm of gold right before being placed in a SEM.

Fly ash–cement mortars were cast at a sand-to-binder ratio of 3 and a water-to-binder ratio of 0.5. Fly ash replacement ratios of 0%, 40% and 60% by mass of cement were selected for mechanical property investigation. Different dosages of CNS (from 0% to 5% by mass of cement plus fly ash) were added to the mixes. Raw materials were dry mixed for 1 min at low speed to obtain a homogenous mix, wet mixed at low speed for another minute, and then mixed at medium speed for 3 min. CNS was hand-stirred in the mixing water prior. After cured in room temperature for 1 day, samples cast in 5 cm (diameter) × 10 cm (length) cylindrical molds were demolded and cured in saturated lime water until testing.

Different water-to-binder ratios were used for pastes (0.4) and mortars (0.5) through this work so as to obtain suitable flowability for each mix, especially for mixes with CNS without superplastizer. Mix proportions of the pastes and mortars are listed in Table 2. To sustain a constant water-to-binder ratio, the replacement of fly ash and addition of CNS were on mass basis, which, however, may bring differences of water volume fraction in mixes with the addition of CNS due to its density difference to that of other powders. The influence of the difference of densities of various powders on the water volume in each fresh mix was calculated by using the densities of the raw materials and the results are shown in Table 2. It demonstrates that the difference of water volume fraction of mixes with and without CNS at the same fly ash replacement ratio is very slight, and thus the influence of water volume difference on the mechanical properties of mixes of the same fly ash replacement ratio is negligible. And the effect of CNS on the mechanical properties of different fly ash replacement systems could be evaluated.

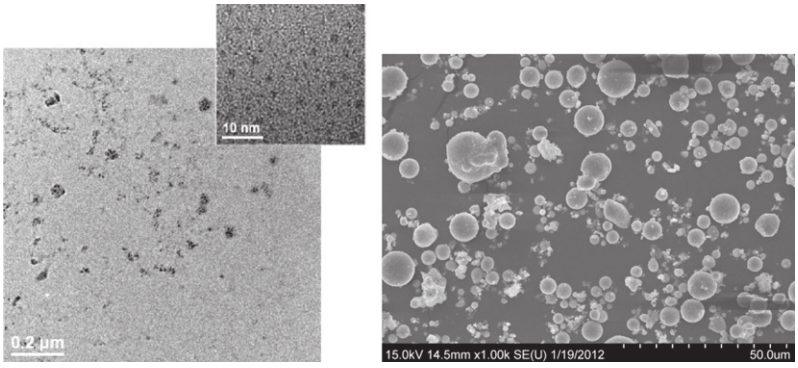

(a) CNS-10nm (TEM) (b) Fly ash (SEM)

Fig. 1. Morphology images of CNS and fly ash.

Table 2
Mix proportions and water volume difference of mixes without and with CNS at the same FA replacement ratio.

FA repl.	Cement (g)	FA (g)	CNS (solid) (g)	Water/g	Water volume fraction (%)	Difference of water volume fraction after CNS addition (%)
Pastes						
0%	100	0	0	40	55.36	0.00
	100	0	5	42	55.01	−0.35
40%	60	40	0	40	52.12	0.00
	60	40	5	42	51.95	−0.17
60%	40	60	0	40	50.64	0.00
	40	60	5	42	50.55	−0.09
Mortars						
0%	100	0	0	50	60.78	0.00
	100	0	5	52.5	60.45	−0.34
40%	60	40	0	50	57.64	0.00
	60	40	5	52.5	57.48	−0.16
60%	40	60	0	50	56.19	0.00
	40	60	0.75	50.38	56.17	−0.01
	40	60	1.5	50.75	56.16	−0.02
	40	60	5	52.5	56.10	−0.09

2.3. Test methods

2.3.1. Compressive strength

The compressive strength of the mortars were measured based on ASTM C109 [27] using a 4448kN MTS hydraulic test machine. For each mix at each age, three 5 cm (diameter) × 10 cm (length) cylindrical samples were tested for assessing the mortar compressive strength. The loading rate of the test was 0.008 mm/s.

2.3.2. Hydration heat

The hydration temperature of each paste was measured by a semi–adiabatic calorimeter. Pastes made with 100 g of binder and 40 g of mixing water (at a temperature of 27 °C) were mixed according ASTM C305 [26], and then cast in 5 cm (diameter) × 10 cm (length) plastic cylinders within 3 min after initial cement and water contact. The sample was then covered and placed in the calorimeter. The calorimeter records the temperature of the sample every 3 min for 20 h. Since the test has a good reproducibility, only one sample was tested for each mix.

2.3.3. Degree of fly ash hydration

The degree of fly ash hydration was determined by the selective dissolving method using 2 N hydrochloric acid. This method is based on the fact that in cement–fly ash pastes, only unhydrated fly ash particles and the non-dissolvable components in cement cannot be dissolved in the 2 N HCl solution [28,29]. By measuring the fly ash amount remaining in the samples dissolved in HCl solution at various hydration ages, the degree of fly ash hydration can be monitored. The dissolving procedure used is the same as that reported in previous research [30], during which 1 g of sample was dissolved in 30 ml of 2 N HCl at 60 °C for 15 min. The undissolved residue was then centrifuged at 4000 rpm. Subsequently the solution was decanted. The solid phase in the centrifuge tube was filled with hot water, centrifuged again at 4000 rpm for 30 s and decanted. This step was repeated three times. Then the residual specimen was dried at 80 °C for 12 h and weighed. The degree of fly ash hydration can be calculated by using the following equations. The hydration degree and non-evaporable water content were calculated based on the ignited samples at 950 °C for 30 min.

$$\alpha = \frac{\left(1 - \frac{\frac{100\times n_{s,HCl}}{100-W_{ne}}}{\frac{40\times n_{FA,HCl}+60\times n_{c,HCl}}{100+W_{CNS}}}\right)\times (R\times n_{FA,HCl} + (1-R)\times n_{c,HCl})}{R\times_{FA,HCl}} \quad (1)$$

$$W_{ne}\% = 100 \times \left[\frac{w_{105^\circ C} - w_{950^\circ C}}{w_{950^\circ C}} - (f_{cem}\times I_c + f_{FA}\times I_{FA} + f_{CNS}\times I_{CNS})\right] \quad (2)$$

where α is the fly ash hydration degree, %; R the fly ash replacement ratio, %; W_{CNS} the CNS dosage, %; W_{ne} the non-evaporable water content, %; I_c the loss of unhydrated cement at 950 °C, %; I_{FA} the loss of fly ash at 950 °C, %; I_{CNS} the loss of CNS at 950 °C, %; $n_{s,HCl}$ the sample undissolved in 2 N HCl, %; $n_{c,HCl}$ the dry cement undissolved in 2 N HCl, which was 8.36%; $n_{FA,HCl}$ the dry fly ash undissolved in 2 N HCl, which was 82.48%; f_{cem} the cement content in the dry mix, which was 57.1%; f_{FA} the fly ash conent in the dry mix, which was 38.1%; f_{CNS} is the CNS powder content in the dry mix, which was 4.8%; note: all the data were % by mass.

An initial study conducted by the authors of this paper has showed that 86% of the CNS is consumed within the first 7 days of hydration, during which the fly ash hydration degree is negligible. Therefore, the pozzolanic reaction of CNS does not overlap with that of fly ash.

2.3.4. $Ca(OH)_2$ content

$Ca(OH)_2$ or CH content of cementitious pastes were assessed using a TGA/sDTA 851 analyzer. Before the tests, samples were dried in an oven at 105 °C for 4 h. During the tests, the weight loss between 440 °C and 510 °C was recorded and considered as the cause of CH decomposition. CH contents were then calculated from this weight loss as a percentage of the remaining weight of the tested sample ignited at 950 °C for 30 min.

2.3.5. Morphology and elemental composition

Hitachi S-4800 FE-SEM equipped with energy dispersive spectroscopy (EDS) was used to analyze the morphology and elemental composition of the pastes. The electron acquisition time, acceleration voltage and acceleration current used were 60 s, 30 KV and 30 μA, respectively. During the test, the areas of interest were magnified to cover the whole area of the monitor screen to avoid the influence of electrons scattered from the vicinity part of area of the interest [31] and then EDS analysis was made. Samples were coated with 20 nm of gold to make it conductive.

Hitachi S-3400 with backscatter electron (BSE) detector was used to analyze the amount of unhydrated cement in pastes. Secontioned samples were polished using silicon carbide paper of

gradation 22 μm, 14.5 μm, and 6.5 μm and the polishing time of each step was 5 min. In the final step, the polished samples were ultrasonically cleaned in water for 1 min using a bath sonicator to remove polishing debris from the sample surface. Then the sample was soaked in acetone for 1 day before being vacuum-dried at 50 °C for 12 h. Samples were also coated with 20 nm of gold. To accurately evaluate the hydration degree, five BSE images were taken from each sample for image analysis, and the results were averaged as the representative value of each sample. At the same time, the smallest magnification as 100× was used to obtain the biggest image that testing equipment could provide.

3. Results and discussions

3.1. Compressive strength

Effects of CNS on the compressive strength of 0%, 40% and 60% fly ash cement mortars are shown in Fig. 2. It reveals that the rate of compressive strength gain of CNS-added mortar is enhanced at early ages and the higher CNS dosage, the greater the enhancement: the compressive strength of 0%, 40% and 60% fly ash mortars are increased by 9%, 50% and 64% at 7 days for the 5% CNS-added cement mortars, respectively. While the enhancement degrees are 10% and 20% for the 0.75% and 1.5% CNS-added cement mortars. However, the strength enhancing effect of CNS gradually becomes smaller and eventually diminishes at later ages and an adverse side effect of CNS can be seen at later ages. It shows that the average compressive strength of mortars with various contents of CNS become smaller with the increase of CNS, and the average strength of control mortar is the highest at 84 days. This trend indicates that the adverse side effect introduced by CNS is more clear when the dosage is higher. Although the early-age strength gain improving effect introduced by 0.75% CNS is smaller than that of 5% CNS, the side effect is negligible at later ages. To explore the reasons for the strength gain characteristics of this system, the early and later age hydration characteristics of fly ash–cement pastes were further evaluated.

3.2. Hydration heat

One of the most significant effects of nanoparticles on cementitious materials is the hydration acceleration effect [32–35]. The effect of CNS on the hydration heat of 40% fly ash cement paste is shown in Fig. 3. It demonstrates that fly ash replacement reduces the hydration peak temperature significantly, and the occurrence of the hydration peak is delayed, as well. Fig. 3 illustrates that with the addition of 5% CNS, an earlier and greater hydration heat peak can be seen in both 20% and 40% fly ash cement pastes, implying a faster and greater degree of hydration.

The hydration acceleration of CNS on cement–fly ash blends is also demonstrated by its effect on the induction period, which lasts from the beginning of hydration to about 2–3 h. During this period, a decrease in temperature was observed due to the low heat generation at this stage. This reveals that the addition of CNS shortens

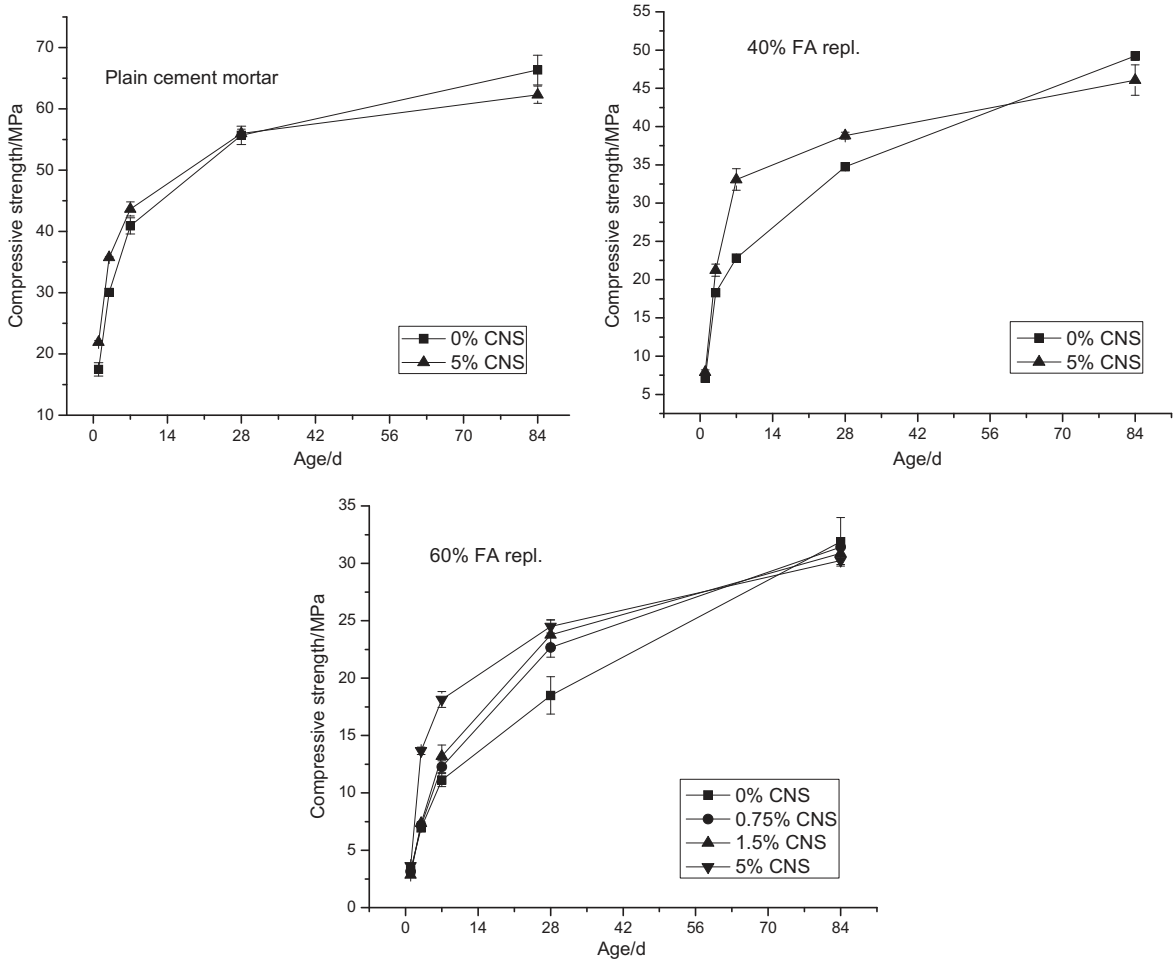

Fig. 2. Effects of CNS on the compressive strength evolution of 0%, 40% and 60% fly ash cement mortar.

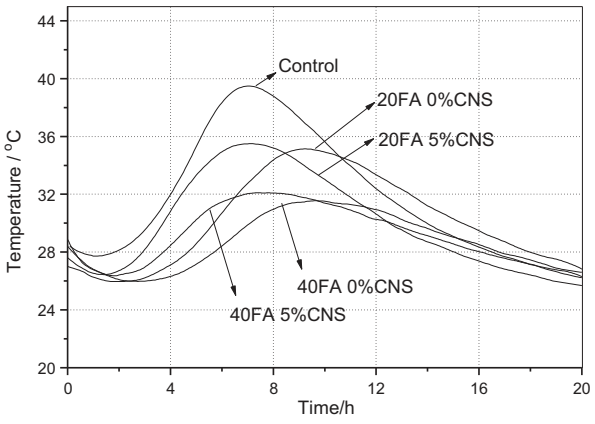

Fig. 3. Effect of CNS on cement–fly ash hydration heat.

the induction period for both 20% and 40% fly ash cement pastes, implying an accelerated hydration of this system.

3.3. Fly ash hydration

Since pozzolanic reaction, from either CNS or FA, has little effect on the total heat of hydration of the cementitious system when compared to cement hydration [34], the effect of CNS on the degree of fly ash hydration is difficult to assess from the calorimetry study. Therefore, chemical dissolving test method was employed in the present study to evaluate the influence of CNS on fly ash hydration.

By measuring the weight of fly ash blends in saturated lime solution, Li [15] observed a higher weight increment rate/degree of nanoSiO_2-added blends and attributed it to the higher pozzolanic reaction of fly ash due to the hydration seeding sites provided by nanoSiO_2. However, the hydration environment in real pastes is different, and the fly ash hydration process may change.

Influence of CNS on the pozzolanic reaction of fly ash is shown in Fig. 4. Significant differences in the hydration characteristics of fly ash are revealed in the CNS-added paste when compared with the hydration characteristics of the FA-cement paste with no CNS. Very little pozzolanic reaction occurs at 7 days in both pastes. However, a slightly higher degree of fly ash hydration is observed in the CNS-added paste. This trend existed for two months, after which the degree of fly ash hydration in CNS-added paste becomes significantly smaller than that of non-CNS paste. Seven months later, the degree of fly ash hydration in non-CNS paste can be as much as 32%, while it is only 18% in 5%CNS paste. This implies that the pozzolanic reaction of fly ash is accelerated in the early age, but the later age reaction is greatly hindered.

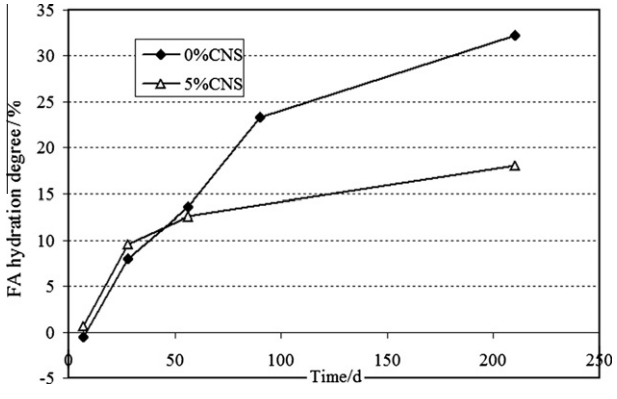

Fig. 4. Effect of CNS on fly ash hydration degree.

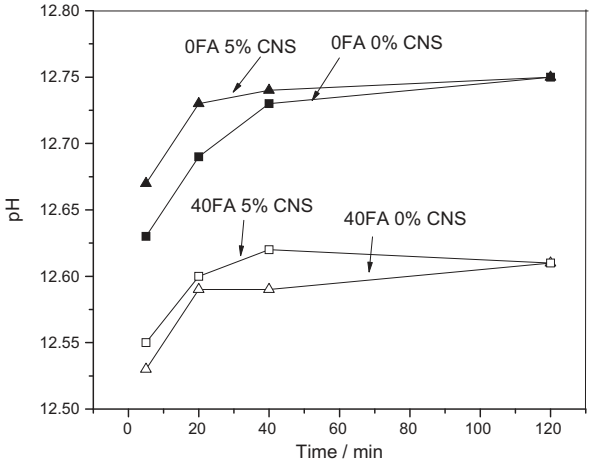

Fig. 5. Effect of CNS on pH value of fly ash cement pastes (w/b = 2).

The pozzolanic reaction of fly ash is highly dependent on the alkalinity of the pore solution [6,36], in which the OH^- breaks the silicate or aluminosilicate network formers in fly ash to form C–S–H gel. And a high pH environment is beneficial for network breakage. This process is illustrated in Eqs. (3) and (4).

$$\equiv Si{-}O{-}Si\equiv + OH^- \rightarrow \equiv Si{-}OH \quad (3)$$

$$\equiv Si{-}OH + Ca(OH)_2 \rightarrow C{-}S{-}H \quad (4)$$

The effect of CNS on the alkalinity of cementitious materials is shown in Fig. 5. It reveals that higher pH values are shown in pastes with 5% CNS before 2 h of hydration in both 0% and 40% fly ash cement pastes. This may be due to the higher cement particle dissolution rate [32].

As aforementioned, pozzolanic reaction is a $Ca(OH)_2$-consuming process. Therefore the evolution of CH content in pastes is a measure of the reaction characteristics of fly ash. Results of the effects of fly ash and CNS on the CH content of cement–fly ash-CNS systems are given in Table 3.

It is shown in Table 3 that the CH contents of 40% fly ash cement pastes are higher than the corresponding calculated values before 28 days, suggesting accelerated cement hydration. This may be due to the higher local water-to-cement ratio caused by the 'dilution effect' of fly ash [28], as well as the heterogeneous hydration nucleation effect of fly ash particles [37]. The lower CH content of the 40% fly ash replacement paste than the calculated value after 28 days is due to the pozzolanic reaction of fly ash.

When comparing the CH contents of the 0% and 5% CNS-added pastes, it reveals that only a slight change in CH content occurs in CNS-added paste from 28 days to 210 days, just from 6.03% to 5.54%. However, a higher reduction in CH content of 1.82% can

Table 3
$Ca(OH)_2$ content in cement–fly ash-CNS systems (% by mass)

Time/d	100% cement	40% FA repl. 0% CNS	40% FA repl. 5% CNS	40% FA repl. 0% CNS (calculated)[a]
1	12.33	8.52	6.85	7.40
3	14.88	10.79	7.23	8.93
7	15.95	10.82	6.28	9.57
28	17.26	11.40	6.03	10.36
56	20.44	8.49	5.77	12.26
210	23.28	9.58	5.54	13.97

[a] Assumed that 40% fly ash has no effect on cement hydration and CH contents were equal to 60% of those produced by 100% cement listed in the second column of this table.

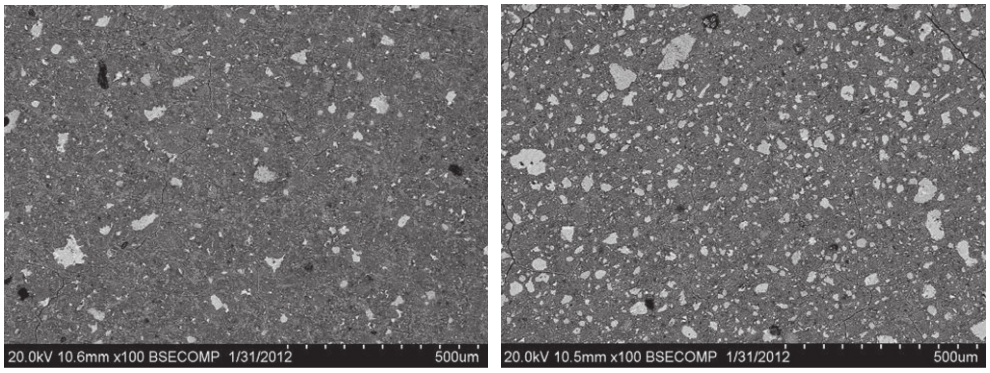

(a) 0% CNS 8months (b) 5% CNS-10 8months

Fig. 6. BSE images of cement pastes.

be seen in non-CNS paste during this period. It implies that the lack of CH is a reason for the hindrance of fly ash hydration in the later age. Moreover, when the effect of CNS on cement hydration is taken into consideration, the CH amount consumed by fly ash at later ages can be higher in 0% CNS-added paste. As revealed in Fig. 6, the unhydrated cement particles in 0% CNS-added paste takes 3.2% of the total area of the image, while the value in the 5% CNS-added paste is 10.6%. The mechanism of this phenomenon is discussed later.

3.4. Microstructure and morphology

The microstructure of CSN-FA-cement pastes was studied under an SEM. Selected secondary electron images are presented in Fig. 7, where the samples are 7 months old.

In the paste with no CNS (Fig. 7a and c), the fly ash particles are coated with significant amount of hydration products, and the uniform rod-like C–S–H gel is tightly packed around fly ash particles. For paste with 5% CNS (Fig. 7b and d), the fly ash particle surface appears very clean and with little features, indicating a lower degree of FA hydration. At the interface between the fly ash particle and the bulk paste, there is a double-layer coating structure (Fig. 7d) in the CNS-added paste. A close examination shows that this coating consists of a hollow tubular layer structure and a compact layer structure (Fig. 7e).

Fig. 8 illustrates the development of this coating structure around a fly ash particle in the 5% CNS-added fly ash–cement paste.

It shows that hydration products are found coating fly ash particles in the 12 h old sample. A clearly compact gel structure, which is about one micron in thickness, can be observed coating the fly ash particles after 7 days, while the bulk gel structure is more porous. Seven months later, the previous porous coating becomes so compact that it can be treated as a uniform layer. This coating layer structure became even more compact at 7 months when compared with that at 7 days. At the same time, a hollow tubular coating of about several hundred nanometers between the unhydrated fly ash particle and the very dense coating is found in the 7 month old sample. It shows that no tubular coating was formed at 7 days and thus it may be deduced that this coating is resulted from hydration of fly ash. Tubular gel structure is prevalent in nature [38,39], and such a hollow tubular gel is considered to be formed following the reverse 'silicate garden' theory. Based on this theory, after contacting with water, a semi-permeable membrane is quickly formed around cement particles, and water and Ca^{2+} diffuses through the membrane while SiO_4^{2+} stays inside. At a certain time, the membrane between the high-silicate and high-calcium solution bursts locally under high osmosis pressure. The jet of the silicate solution, which erupts into the calcium solution, precipitates continuously to form a tube of solid hydrates [40,41].

From the distinct morphology of the coating structure, it may be expected to be due to the pozzolanic reaction and the cement hydration acceleration effect of CNS. The accelerated formation of C–S–H gel at the early age covering the fly ash particles may act as an ion transportation barrier, thus hinders fly ash hydration later on. A similar cement hydration hindrance mechanism was also found in fresh paste cured at high temperatures. It has been well-documented that the early-age hydration and hardening properties of cement-based materials can be improved by high temperature curing. However, both properties in the later age can be adversely affected [42,43]. This has been tied to the C–S–H gel that forms around the cement particles at early ages, which has no sufficient time to diffuse and forms a well-compacted layer that acts as a barrier of ion penetration and hinders cement hydration at later ages [42,44,45]. However, for the gel formed under normal and low temperatures, no such hydrate coating is formed [43]. Verbeck and Helmuth [45] suggested that at low temperatures there is more time for the hydration products to diffuse than at higher temperatures.

Effects of coating formed at early-ages on unhydrated cement particles in high temperature was also shown by its effect on the microstructure: it has been reported that although C–S–H near the cement grain is much denser and stronger in high temperature cured samples, the cement bulk matrix is more homogenous and less porous for samples cured at low temperatures [43,46] and thus the compressive strength is higher [47]. A lower degree of cement hydration as shown in Fig. 6 and highly porous microstructure as reported in nanoSiO_2-added cement paste [48] may contribute to the lowered strength gain rate in the later age as shown in Fig. 2.

To identify the chemical characteristics of the coating around FA particles in the CNS-added paste, EDS analysis was conducted in both the coating and bulk paste regions. Fig. 9 shows the elemental compositions of the compact coating and the C–S–H gel in the bulk paste region, where one mark represents one data point obtained from one spot tested. As seen in the figure, the mean Ca/Si ratio of the FA coating and the bulk C–S–H gel are 1.38 and 1.68, respectively. It has been reported that C–S–H gel with a low Ca/Si ratio is less permeable [49], thus it is deduced that beyond the compacted gel structure, the chemical composition of coating may also contribute to the delayed hydration of fly ash in the later age.

3.5. Further discussions

The above test results and discussions have deduced that a quick formation of C–S–H gel resulting from both CNS hydration

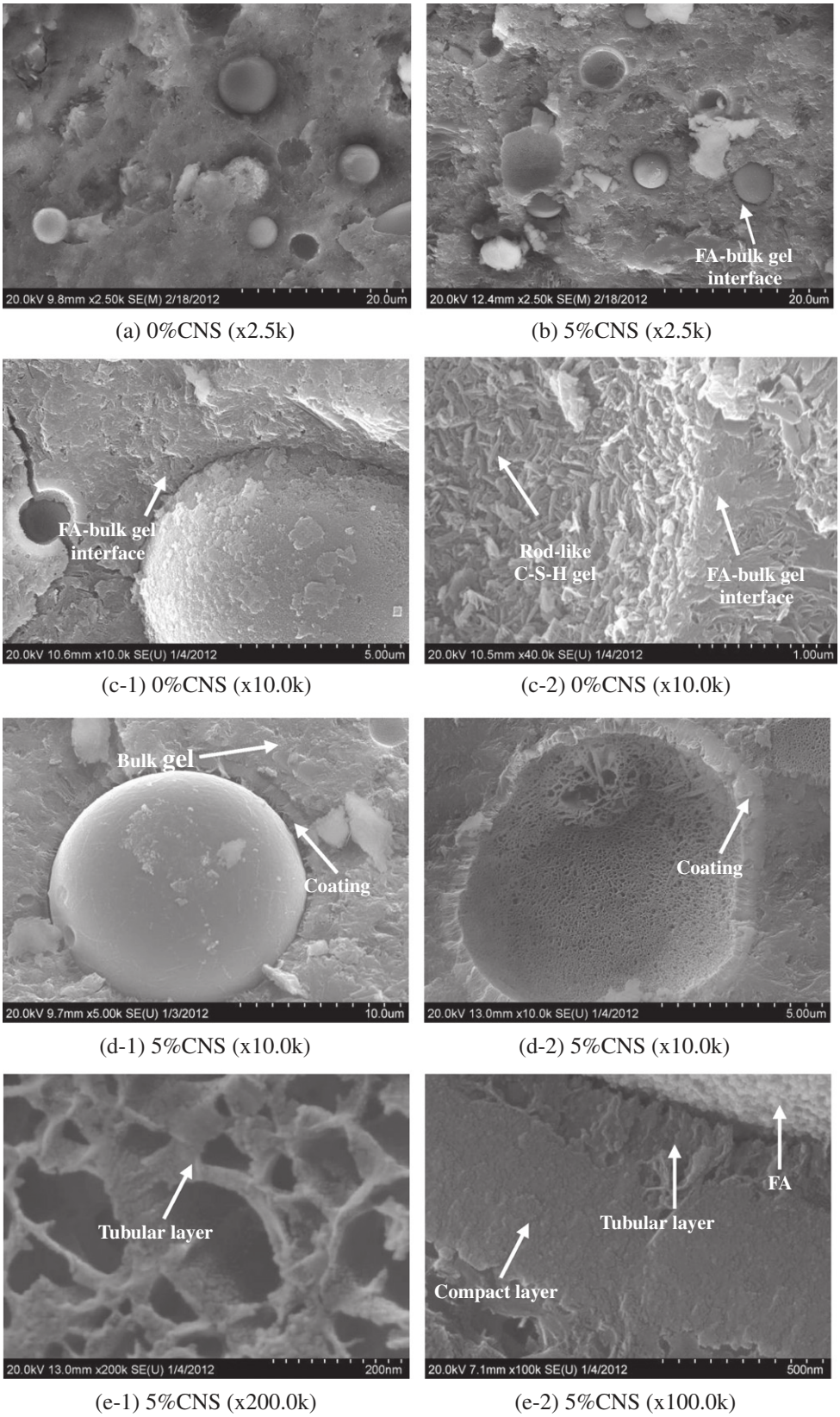

Fig. 7. SEM images of FA-cement paste without and with CNS addition at 7 months.

and accelerated cement hydration at early age can have an adverse effect on the hydration property of cementitious materials at later age. This is because abundant hydration products formed around the cementitious material particles become denser with time and prevent the cementitious materials from further hydration at later age. These results suggest that the highly reactive nanoSiO_2 would enhance hydration of cementitious materials at early age but may not be beneficial for the strength development at later age. This

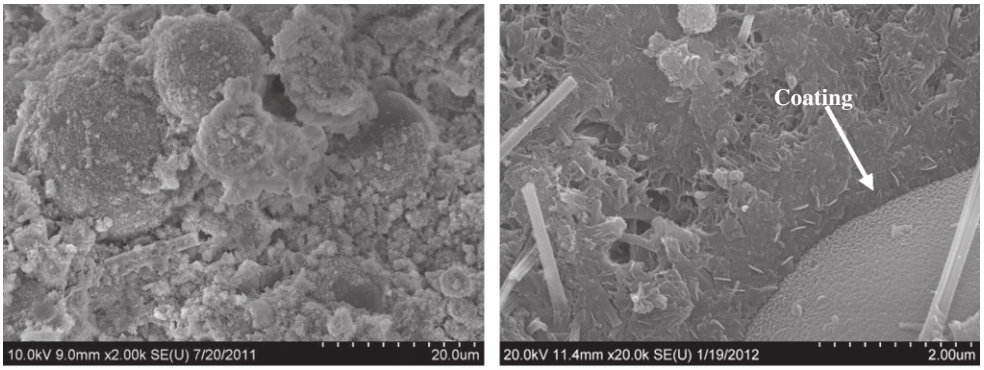

(a) 12 hours (b) 7 days

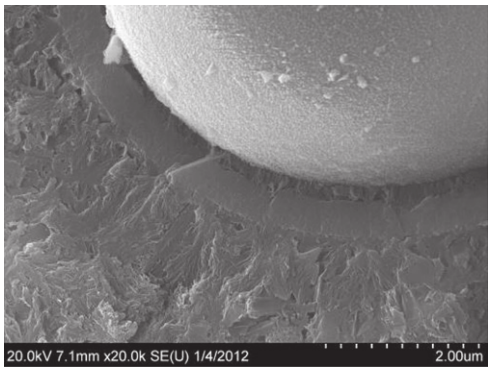

(c) 7months

Fig. 8. Development of the layer structure around a fly ash particle in the 5% CNS-added fly ash–cement paste.

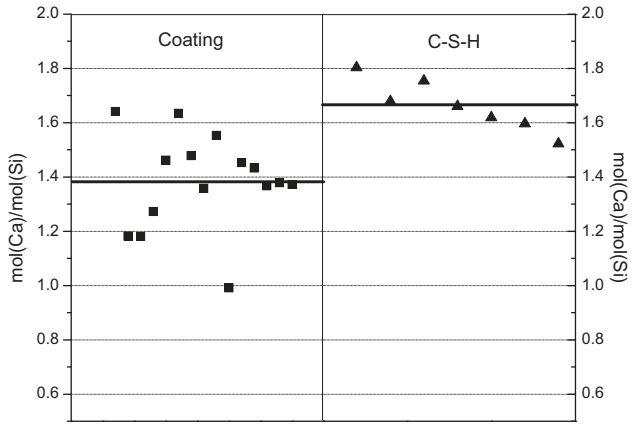

Fig. 9. Ca/Si ratio comparison of compact coating and the bulk C–S–H gel.

influence may be more significant for finer nanoparticles. If the nanoparticles are CH-consuming materials, hydration of pozzolanic materials at later age may be more impaired since little CH is available and the CH is difficult to reach the surface of the pozzolanic materials because of the dense coating formed around them. In addition, nanoparticles may tend to adhere to cementitious material particles and result in more C–S–H gel formed around them and prevent them from further hydration at late age. This may explain why the cementitious materials with smaller-sized nanoSiO_2 had a lower strength gain at later age [50]. From the hydration hindrance mechanism discussed above, it can be deduced that cement hydration hindrance effect may be eliminated by using finer cement particles [51] and smaller amount of nanoSiO_2, although the latter may sacrifice the very early-age strength gain improving effect, as shown in Fig. 2. Considering the electronegativity of hydrated calcium silicate and electropositivity of nanoSiO_2 [52,53], the adsorption of nanoSiO_2 on hydrated cement particles may be alleviated when it is surfactant-treated [53] and then less hydration product may be formed on unhydrated cement particles.

4. Conclusions

The main conclusions from this work are as follows:

(1) The early age strength gain of a CNS-added FA-cement paste is probably due to the acceleration effect of nanoSiO_2 on both cement and fly ash hydration.
(2) Although CNS can enhance the pozzolanic reaction of fly ash by increasing the alkalinity of solution in the early age, its later age hydration may be adversely affected.
(3) There is a dense coating around FA particles in the CNS-added pastes, which, with a low Ca/Si ratio may result from the reactive CNS hydration at the early age and act as a barrier that hinders ion penetration and consequently the fly ash hydration at the later age.

It is recommended that the accelerating and adverse effects of nanoSiO_2 on hydration of cementitious materials at both early and later ages as well as the influence of nanoSiO_2 hydration on the gel morphology of the FA-cement pastes shall be considered together so as to properly use nanoSiO_2 in cement-based materials. At the same time, methods of alleviating the hydration hindrance effects of nanoSiO_2 at later ages need to be explored.

Acknowledgements

The authors would like to acknowledge the financial support from Infrastructure Technology Institute at Northwestern

University under Grant DTRT06-G-0015 and Tennessee Valley Authority (TVA) and Oak Ridge Associated Universities (ORAUs) (Award 105866). The first author would also like to thank China Scholarship Council for its financial support during his study at Northwestern University.

References

[1] Hassett D, Eylands K. Heat of hydration of fly ash as a predictive tool. Fuel 1997;76(8):807–9.
[2] Lam L, Wang Y, Poon C. Degree of hydration and gel/space ratio of high-volume fly ash/cement systems. Cem Concr Res 2000;30(8):747–56.
[3] Sakai E, Miyahara S, Ohsawa S, Lee S, Daimon M. Hydration of fly ash cement. Cem Concr Res 2005;35(6):1135–40.
[4] Ati C. Heat evolution of high-volume fly ash concrete. Cem Concr Res 2002;32(5):751–6.
[5] Payá J, Monzo J, Borrachero M, Peris-Mora E. Mechanical treatment of fly ashes: Part IV. Strength development of ground fly ash-cement mortars cured at different temperatures. Cem Concr Res 2000;30(4):543–51.
[6] Qian J, Shi C, Wang Z. Activation of blended cements containing fly ash. Cem Concr Res 2001;31(8):1121–7.
[7] Babaian P, Wang K, Mishulovich A, Bhattacharja S, Shah S. Effect of mechanochemical activation on reactivity of cement kiln dust–fly ash systems. J ACI Mat 2003;100(1):55–62.
[8] Goñi S, Guerrero A, Luxán M, Macías A. Activation of the fly ash pozzolanic reaction by hydrothermal conditions. Cem Concr Res 2003;33(9):1399–405.
[9] Wang K, Shah S, Mishulovich A. Effects of curing temperature and NaOH addition on hydration and strength development of clinker-free CKD-fly ash binders. Cem Concr Res 2004;34(2):299–309.
[10] Langan B, Wang K, Ward M. Effect of silica fume and fly ash on heat of hydration of Portland cement. Cem Concr Res 2002;32(7):1045–51.
[11] Khedr S, Abou Zaid M. Characteristics of silica-fume concrete. J Mat Civ Eng 1994;6(3):357–74.
[12] Malhotra V, Carette G. An efficient material: silica fume concrete-properties, applications, and limitations. J ACI Mat 1983;5(5):40–6.
[13] Ye Q, Zhang Z, Kong D Kong. Influence of nano-SiO_2 addition on properties of hardened cement paste as compared with silica fume. Constr Build Mat 2007;21(3):539–45.
[14] Jo B, Kim C, Lim J. Characteristics of cement mortar with nano-SiO_2 particles. Constr Build Mat 2007;21(6):1351–5.
[15] Li G. Properties of high-volume fly ash concrete incorporating nano-SiO_2. Cem Concr Res 2004;34(6):1043–9.
[16] Said A, Zeidan M. Enhancing the reactivity of normal and fly ash concrete using colloidal nano-silica. Am Concr Inst, ACI Special Publication 2009;267:75–86.
[17] Zhang M, Islam J. Use of nano-silica to reduce setting time and increase early strength of concretes with high volumes of fly ash or slag. Constr Build Mat 2012;29:573–80.
[18] Zhang M, Islam J, Peethamparan S. Use of nano-silica to increase early strength and reduce setting time of concretes with high volumes of slag. Cem Concr Comp 2012;34:650–62.
[19] Nazari A, Riahi S. The effects of zinc dioxide nanoparticles on flexural strength of self-compacting concrete. Composites Part B: Eng 2011;42(2):167–75.
[20] Sato T, Diallo F. Seeding effect of nano-CaCO3 on the hydration of tricalcium silicate. Transp Res Rec 2010; (2141):61–7.
[21] Jo B, Kim C, Lim J. Characteristics of cement mortar with nano-SiO_2 Particles. J ACI Mat 2007;104(4):404–7.
[22] Senff L, Dachmir H, Wellington L, Repette WL, Ferreira V, Labrincha J. Mortars with nano-SiO_2 and micro-SiO_2 investigated by experimental design. Constr Build Mat 2010;24:1432–7.
[23] Nazari A, Riahi S. The effects of SiO_2 nanoparticles on physical and mechanical properties of high strength compacting concrete. Composites Part B: Eng 2011;42(3):570–8.
[24] Richardson I. The nature of C–S–H in hardened cements. Cem Concr Res 1999;29:1131–47.
[25] <http://www.mknano.com/item-details.asp?catDisp=2&itemid=80&id=10>. MK Impex Corporation, Canada.
[26] ASTM C305–2011. Standard practice for mechanical mixing of hydraulic cement pastes and mortars of plastic consistency. ASTM International, West Conshohocken, PA, USA; 2008.
[27] ASTM C109–08. Standard test method for compressive strength of hydraulic cement mortars (Using 2-in. or [50-mm] cube specimens). ASTM International, West Conshohocken, PA, USA; 2008.
[28] Zeng Q, Li K, Fen-chong T, Dangla P. Determination of cement hydration and pozzolanic reaction extents for fly-ash cement pastes. Constr Build Mat 2012;27(1):560–9.
[29] Ohsawa S, Asaga K, Goto S, Daimon M. Quantitative determination of fly ash in the hydrated fly ash - $CaSO_4{\cdot}2H_2O$-$Ca(OH)_2$ system. Cem Concr Res 1985;15(2):357–66.
[30] Termkhajornkit P, Nawa T, Nakai M, Saito T. Effect of fly ash on autogenous shrinkage. Cem Concr Res 2005;35(3):473–82.
[31] Scrivener K. Backscattered electron imaging of cementitious microstructures: understanding and quantification. Cem Concr Comp 2004;26(8):935–45.
[32] Mija H, Thomas J, Jennings H. Influence of nucleation seeding on the hydration kinetics and compressive strength of alkali activated slag paste. Cem Concr Res 2011;41(8):842–6.
[33] Alizadeh R, Raki L, Makar L, Beaudoin J, Moudrakovski I. Hydration of tricalcium silicate in the presence of synthetic calcium-silicate-hydrate. J Mat Chem 2009;19(42):7937–46.
[34] Thomas J, Jennings M, Chen J. Influence of nucleation seeding on the hydration mechanisms of tricalcium silicate and cement. J Phys Chem 2009;113(11):4327–34.
[35] Sato T, Beaudoin J. The Effect of nano-sized $CaCO_3$ addition on the hydration of cement paste containing high volumes of fly ash. In: 12th international congress on the chemistry of cement, Montreal, QC; 2007. p. 1–12.
[36] Li D, Chen Y, Shen J, Su J, Wu X. The influence of alkalinity on activation and microstructure of fly ash. Cem Concr Res 2000;30(6):881–6.
[37] Lawrence P, Cyr M, Ringot E. Mineral admixtures in mortars: effect of inert materials on short-term hydration. Cem Concr Res 2003;33(12): 1939–47.
[38] Pratama F, Robinson H, Pagano J. Spatially resolved analysis of calcium–silica tubes in reverse chemical gardens. Colloids Surf A: Physicochem Eng Aspects 2011;389(1–3):127–33.
[39] Barnes P, Ghose A, Mackay A. Cement tubules — another look. Cem Concr Res 1980;10(5):639–45.
[40] Coatman R, Thomas N, Double D. Studies of the growth of "silicate gardens" and related phenomena. J Mat Sci 1980;15:2017–26.
[41] Double D. The hydration of Portland cement. Nature 1976;261:486–8.
[42] Escalante-García J, Sharp J. The microstructure and mechanical properties of blended cements hydrated at various temperatures. Cem Concr Res 2001;31(5):695–702.
[43] Escalante-García J, Sharp J. Effect of temperature on the hydration of the main clinker phases in Portland cements: part I, neat cements. Cem Concr Res 1998;28(9):1245–57.
[44] Lothenbach B, Winnefeld F, Alder C, et al. Effect of temperature on the pore solution, microstructure and hydration products of Portland cement pastes. Cem Concr Res 2007;37(4):483–91.
[45] Verbeck G, Helmuth R. Structures and physical properties of cement paste. In: Proc 5th Int Symp Chem Cem 1968; 3: 1–32.
[46] Bentur A. Effect of curing temperature on the pore structure of tricalcium silicate pastes. J Coll Interface Sci 1979;74(2):549–60.
[47] Knut O, Kjellsen R, Gjørv O. Backscattered electron imaging of cement pastes hydrated at different temperatures. Cem Concr Res 1990;30(2):308–11.
[48] Thomas J, Jennings H. The nanostructure of low-CO_2 Concrete for a sustainable infrastructure. In: Report on year 1 activities and recommendations for future work, a scientific collaboration between Lafarge Center for Research (LCR) and Northwestern University (NWU); 2010.
[49] Garrault S, Nonat A. Hydrated layer formation on tricalcium and dicalcium silicate surfaces: experimental study and numerical simulations. Langmuir 2001;17(26):8131–8.
[50] Givi A, Riahi S, Aziz F. Experimental investigation of the size effects of SiO_2 nano-particles on the mechanical properties of binary blended concrete. Composites Part B 2010;41:673–7.
[51] Garrault S, Behr T, Nonat A. Formation of the C–S–H Layer during early hydration of tricalcium silicate grains with different sizes. J Phys Chem Part B 2006;110(1):270–5.
[52] Nägele E, Schneider U. The zeta-potential of cement: Pt. V: effect of surfactants. Cem Concr Res 1988;18(2):257–64.
[53] Lee C, Lo L, Mou C, Yang C. Synthesis and characterization of positive-charge functionalized mesoporous silica nanoparticles for oral drug delivery of an anti-inflammatory drug. Adv Funct Mat 2008;18:3283–92.